Visual Neuroscience (2003), **20**, 351–361. Printed in the USA.

DOI: 10.1017/S0952523803204016

Inhibitory network properties shaping the light evoked responses of cat alpha retinal ganglion cells

BRENDAN J. O'BRIEN,* RANDAL C. RICHARDSON, AND DAVID M. BERSON

Department of Neuroscience, Brown University, Box 1953, Providence

(RECEIVED August 16, 2002; ACCEPTED June 16, 2003)

Abstract

Cat retinal ganglion cells of the Y (or alpha) type respond to luminance changes opposite those preferred by their receptive-field centers with a transient hyperpolarization. Here, we examine the spatial organization and synaptic basis of this light response by means of whole-cell current-clamp recordings made *in vitro*. The hyperpolarization was largest when stimulus spots approximated the size of the receptive-field center, and diminished substantially for larger spots. The hyperpolarization was largely abolished by bath application of strychnine, a blocker of glycinergic inhibition. Picrotoxin, an antagonist of ionotropic GABA receptors, greatly reduced the attenuation of the hyperpolarizing response for large spots. The data are consistent with a model in which (1) the hyperpolarization reflects inhibition by glycinergic amacrine cells of bipolar terminals presynaptic to the alpha cells, and perhaps direct inhibition of the alpha cell as well; and (2) the attenuation of the hyperpolarization by large spots reflects surround inhibition of the glycinergic amacrine by GABAergic amacrine cells. This circuitry may moderate nonlinearities in the alpha-cell light response and could account for some excitatory and inhibitory influences on alpha cells known to arise from outside the classical receptive field.

Keywords: Retina, Retinal ganglion cell, Gamma amino butyric acid (GABA), Glycine, Amacrine cell

Introduction

Retinal ganglion cells (RGCs) are the output neurons of the retina with connections to many central brain nuclei. Mammalian ganglion cells are divisible into a large number of cell types, distinguishable on the basis of their unique morphological and physiological characteristics (for review see: Rowe & Stone, 1977; Rodieck & Brening, 1983; Stone, 1983; Wässle & Boycott, 1991; Cook, 1997; Rodieck, 1998; Dacey, 1999; Troy & Shou, 2002). Perhaps the most widely studied RGC type is known as the alpha or Y cell. Originally described in cat retina (Enroth-Cugell & Robson, 1966; Boycott & Wässle, 1974), these cells are apparently present in most, if not all, mammalian retinae (Peichl, 1991). They have very large cell bodies; thick, rapidly conducting axons; and widely spreading, radiate dendritic arbors. Their receptive fields are correspondingly large, exhibit a conventional center-surround organization, and are subdivided into either ON or OFF subtypes depending on their sign of preferred contrast. ON-center alpha cells have a dendritic arborization in sublamina *b* of the inner plexiform layer (IPL) and are excited by luminance increments in their receptive-field center. OFF-center alpha cells arborize in sublamina *a* of the IPL and are excited by luminance decrements. Both subtypes respond relatively transiently to luminance steps and summate luminance information nonlinearly. They are more sensitive to luminance contrast than many other RGC types and respond better to rapid stimulus motion (for review, see Troy & Shou, 2002).

Most studies of alpha-cell light responses have utilized extracellular recording techniques. Postsynaptic potentials (PSPs) underlying the patterning of spike discharge, particularly inhibitory PSPs (IPSPs), have not been studied in great detail. We have taken advantage of new retinal recording techniques (Taylor & Wässle, 1995; Robinson & Chalupa, 1997; O'Brien et al., 2002) to obtain whole-cell patch-clamp recordings of cat alpha-cell light responses. In addition, use of pharmacological blockers of the inhibitory neurotransmitters GABA and glycine allowed us to identify the roles they play in shaping alpha-cell light responses. Our data suggest that alpha-cell hyperpolarization in response to nonpreferred light stimuli is mediated largely through narrow-field glycinergic amacrine cells. Further pharmacological experiments demonstrated that these glycinergic amacrine cells are under the influence of wide-field GABAergic amacrine cells. The interactions of these two inhibitory networks may play a role in adapting the retina for optimal processing of different spatial frequencies.

Address correspondence and reprint requests to: David M. Berson, Department of Neuroscience, Brown University, Box 1953, Providence, RI 02912-1953, USA. E-mail: David_Berson@brown.edu

*Present address: Department of Optometry and Visual Science, University of Auckland, Private Bag 92019, Auckland, New Zealand.

Methods

Data come from 11 pigmented domestic cats ranging in age from 4 months to adulthood. Methods conformed with NIH guidelines and were approved by the Brown University Institutional Animal Care and Use Committee (IACUC). Animals were sedated with a mixture of acepromazine (2.5 mg, i.m.) and atropine sulfate (0.14 mg, i.m.), and deeply anesthetized with Nembutal (50 mg, i.v., supplemented as necessary). Preparation of retina–retinal pigment epithelium–choroid tissue blocks and whole-cell patch-clamp recording were as in O'Brien et al. (2002). Briefly, one ocular quadrant of the tissue preparation was mounted in the chamber and continuously superfused during recording (2–5 ml/min) with carbogenated Ames medium (room temperature, ~22°C) supplemented with 22.6 mM sodium bicarbonate and 10 mM D(+)-glucose. To visualize ganglion cells, the retina was stained dropwise with the vital dye acridine orange (0.03% in Ames medium). Alpha cells were selected on the basis of their large soma size (>25 μm, Boycott & Wässle, 1974). Their somatic plasma membrane was exposed for whole-cell patch-clamp recording by mechanical removal of overlying tissue as previously described (O'Brien et al., 2002). Cells with granulated cytoplasm were avoided. The internal solution of the micropipette consisted of (in mM) $KMeSO_4$ 130, NaCl 5, KCl 4, EGTA 0.5, HEPES 10, ATP-Mg 4, phosphocreatine 7, and GTP-Tris 0.3; (mOsm = 280, pH = 7.3, $E_{Cl} = -57$ mV). Lucifer Yellow (0.1%, dipotassium salt; Sigma Chemical Co., St. Louis, MO) and biocytin (0.5%) were included in the internal solution to permit histological confirmation of alpha-cell morphology.

Drugs added to the superfusate included picrotoxin (PTX, 50–100 μM; RBI, Natick, MA), strychnine hydrochloride (SRY 0.3 μM; Sigma), SR-95531 (6 μM, RBI), and hexamethonium bromide (HEX 100 μM; Sigma). All drugs were prepared and stored in accordance with manufacturer's recommendations and applied in concentrations commonly utilized in mammalian retina. Drug effects were generally noted within ~30–60 s and data acquisition began 3–5 min following drug onset. Washout of drugs was performed after each pharmacological condition. SRY effects were invariably and readily reversible on washout. PTX effects were at least partially reversible, but because washout was slow, reversibility was usually incomplete.

Physiological data collection

Whole-cell current-clamp recordings from retinal ganglion cells were obtained with standard procedures (Hamill et al., 1981) using an intracellular amplifier (Neurodata/Delaware Water Gap, PA, DR-886). Voltage-clamp recordings were not attempted due to the inherent space-clamp problems associated with alpha cells, which have very low input resistance and large dendritic fields (O'Brien et al., 2002). Initial pipette resistance ranged between 3 and 7 MΩ. The pipette voltage in the bath was nulled prior to recording. It was also checked immediately after each recording after clearing the pipette tip with a pulse of pressure. After obtaining a gigaohm seal and rupturing the cellular membrane, the pipette series resistance was measured and compensated with the bridge balance circuit of the amplifier. Resting potentials (mean = −66 mV ± 4.2 S.D.) were corrected for the change in liquid junction potential that occurs upon break-in and cell dialysis (−13 mV, Neher, 1992). Cells were excluded from analysis if they exhibited marked instability of resting potential. No capacitance compensation was employed. As antagonism of inhibitory neurotransmission frequently caused a general depolarization and an increased firing rate, hyperpolarizing current was typically administered to counteract the steady depolarization. Voltage and injected current records and logic pulses marking stimulus events were digitized at 2 kHz (AT-MI0-16E-10, National Instruments, Austin, TX), stored in digital format for off-line analysis, and analyzed with custom software developed using Labview 5.0 (National Instruments) or Excel 2002 (Microsoft).

Visual stimulus

The stimulus was generated by a programmable graphics card (SGT+, Number Nine Computer Corp., Lexington, MA) in an IBM AT computer and displayed on a 5-inch monochrome VGA monitor (MO-7500, Siliconrax, Sunnyvale, CA; 640 × 480 pixels; 60 Hz vertical refresh rate). The display screen lay at the film plane of the microscope's camera port and was focused on the photoreceptor layer through a 4× objective. The dichroic filter used for epifluorescence detection of acridine orange and Lucifer yellow (Olympus BH2-DMBG, O-515, Tokyo, Japan) remained in the light path and attenuated the short-wavelength end of the visible spectrum (<515 nm). Mean luminance corresponded to approximately 40,000 photoisomerizations/cone/s, near the transition between the cat's mesopic and photopic ranges (Enroth-Cugell et al., 1977).

Receptive fields were first plotted manually using flashed spots. The computer then presented a series of ten spots (approximately 60% Michelson contrast) centered on the receptive field and ranging in diameter from 0.14 mm to 2.8 mm, corresponding to 0.6 deg to 12.4 deg of visual angle (4.4 deg/mm, Bishop et al., 1962). Stimulus durations were fixed within a series, identical to the interstimulus interval, and ranged from 3 s to 5 s across series. Stimulus series were repeated 2–5 times to obtain average records. Recordings typically lasted 1–2 h.

Immunocytochemistry and morphological identification

Before withdrawing the pipette, the cell was inspected for Lucifer Yellow fluorescence and, if necessary, negative current was injected to increase the intracellular concentration of dye. The tissue was removed from the chamber, mounted onto nylon filter paper (Osmonics, Minnetonka, MN, #R02SP04700), fixed for 2–3 h in buffered 4% paraformaldehyde, and stored for up to 2 weeks in 0.1 M phosphate- buffered saline (PBS) at 4°C. Intracellular staining was revealed with Lucifer Yellow immunoreactivity (Pu & Berson, 1992). Subsequent microscopic inspection (Olympus BH-2) confirmed that all recorded cells were alpha cells.

Data analysis

Dimensions of receptive-field centers were estimated as the size of the preferred contrast spot evoking the largest depolarization at onset. Resting membrane potential (V_r) was defined as the mean voltage during 500 ms prior to each visual stimulus (Fig. 1). To evaluate the underlying postsynaptic potentials more clearly, action potentials were digitally removed from each record. Except during measurement of membrane conductance, where smoothing would significantly alter the shape of the trace during current injection, traces were smoothed by averaging over 50-ms epochs.

Alpha-cell light responses were quantified by separating them into depolarizing and hyperpolarizing compartments (Fig. 1). During presentation of a preferred light stimulus (Fig. 1, stippled

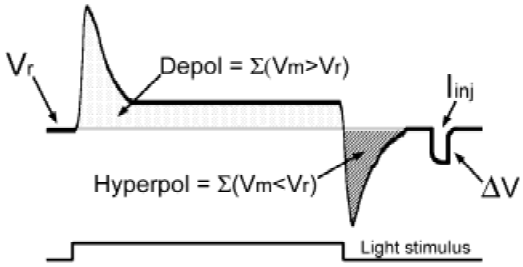

Fig. 1. Diagram of alpha-cell light response quantification. V_r = resting membrane potential. Depol = measurement of alpha-cell depolarization during light stimulus presentation. Hyperpol = measurement of alpha-cell hyperpolarization following termination of light stimulus. *I*inj = time of current injection, ΔV = voltage deflection measured as a consequence of current injection. See Methods for further details.

region), the membrane voltage (V_m) was compared with the resting membrane voltage (V_r) and those values greater than V_r were summed to yield a measurement of depolarization. Termination of a preferred light stimulus led to membrane hyperpolarization beyond rest, and values less than V_r were summed to obtain a measurement of cellular hyperpolarization (Fig. 1, hatched). In some cases, stimulus termination led to an initial hyperpolarization followed by a secondary depolarization (see Results). This secondary depolarization was quantified in the same manner as the depolarization evoked by preferred contrast steps. Each of these variables (depolarization, hyperpolarization, and secondary depolarization) was then plotted individually with respect to spot size to obtain three area-response functions. Because of the vast differences in the relative amplitudes of these response variables, they were normalized to their individual maxima for ease of comparison. To allow averaging of area-response functions across cells with different receptive-field sizes, the expression of stimulus size was normalized by expressing them as a percentage of the *optimal* spot diameter. Data points were then binned (0–49% preferred, 50–99%, 100%, 100–175%, 176–250%, 251–325%, and 326+%) and averaged.

Results

Components of light-evoked PSPs in alpha cells

We examined the responses of ON ($n = 5$) and OFF ($n = 10$) alpha (Y) cells to light or dark spot stimuli of various sizes (Fig. 2). Recordings were made primarily in the retinal periphery, and receptive-field centers were accordingly large (mean diameter: 3.6 deg ($\pm$1.1 S.D.), approximately 820 μm). The left pair of panels of Fig. 2 show the response of an OFF alpha cell (Fig. 2A) and an ON alpha cell (Fig. 2C) to spots of appropriate contrast. For convenience, such stimuli (light for ON alphas, dark for OFF alphas) will be termed "preferred contrast" stimuli. Spots of preferred contrast and of optimal size evoked an initial transient depolarization followed by a smaller sustained component that was maintained throughout stimulus presentation. Termination of such stimuli evoked a prominent hyperpolarization lasting 0.2–1.1 s.

The voltage profile evoked by preferred-contrast stimuli was essentially inverted when the spot's sign of contrast was mismatched to the cell's center type. Such stimuli, here termed "nonpreferred" (dark for ON alphas, light for OFF alphas), evoked a marked hyperpolarization with a large initial transient at stimulus onset and, when extinguished, a transient depolarization (Figs. 2B & 2D). The hyperpolarizing response evoked in alpha cells by a nonpreferred luminance change (disappearance of a preferred stimulus or onset of a nonpreferred stimulus) is the primary focus of this report.

Dependence of the hyperpolarization on glycinergic inhibition

To explore the synaptic basis of this hyperpolarizing response, we examined the effects of antagonists of GABA and glycine, the major inhibitory neurotransmitters in the IPL. Bath application of the glycine receptor antagonist strychnine (SRY, 0.3 μM) largely abolished the initial hyperpolarization. An example is shown in Fig. 3A(i). In this ON alpha cell, the onset of a dark spot of optimal size (a nonpreferred stimulus) evoked, in control conditions (CNTL), a marked transient hyperpolarization. Strychnine (SRY; gray trace) almost completely eliminated this transient hyperpolarization. In its place, a small transient depolarization was observed, followed by a return to a sustained hyperpolarization lasting for the duration of the stimulus. This attenuation by strychnine of the transient hyperpolarization induced by nonpreferred luminance steps was observed among all alpha cells tested, whether ON or OFF center and whether triggered by the onset of nonpreferred stimuli or by the termination of preferred stimuli (not illustrated; but compare Fig. 3A(ii)). On average, strychnine reduced the integrated amplitude of the transient hyperpolarization to less than 25% of its maximum control value (Fig. 3C; triangles). Similar effects were observed when we considered the peak rather than the integrated amplitude of the hyperpolarization (Fig. 3D). There were two hyperpolarizing potentials that persisted in the presence of strychnine. The first, seen in many cells, was a very brief hyperpolarization (see Fig. 3A; PTX/SRY) corresponding to the initial phase of the hyperpolarization evident under control conditions. The second was a very sustained hyperpolarization, evident throughout the nonpreferred stimulus presentation (Fig. 3A(i), *).

A GABAergic mechanism conferring size selectivity on the hyperpolarizing mechanism

The hyperpolarization evoked by nonpreferred luminance steps was strongly dependent on stimulus size. For spots restricted to the receptive-field center, the hyperpolarization increased in amplitude with increases in spot size (see first three traces in each panel of Fig. 2). The maximal hyperpolarization was obtained with spots 4.17 $\pm$ 1.46 deg (mean $\pm$ S.D.), slightly larger than the estimated center diameter (3.61 $\pm$ 1.11 deg) in the same cells. As spots increased in size beyond the center, the evoked hyperpolarization was progressively reduced in amplitude and duration. This can be observed in Fig. 2 by comparing the middle and bottom traces in each panel. The size dependence is shown more clearly for another ON alpha cell in Fig. 3B(i), which overlays the hyperpolarizations evoked when light spots centered on its receptive field, but varying in size, were extinguished. A spot roughly matched in size to the center (4.6-deg diameter) evoked a much larger hyperpolarization than did spots extending substantially beyond the center (7.3 deg and 11.2 deg). Population data summarizing the effect of spot size on the integrated hyperpolarization appear in Fig. 3C (circles). Similar, though somewhat less dramatic, size dependence of the hyperpolarization was evident when considering its peak amplitude (Fig. 3D). The data of Figs. 3C and 3D were derived from

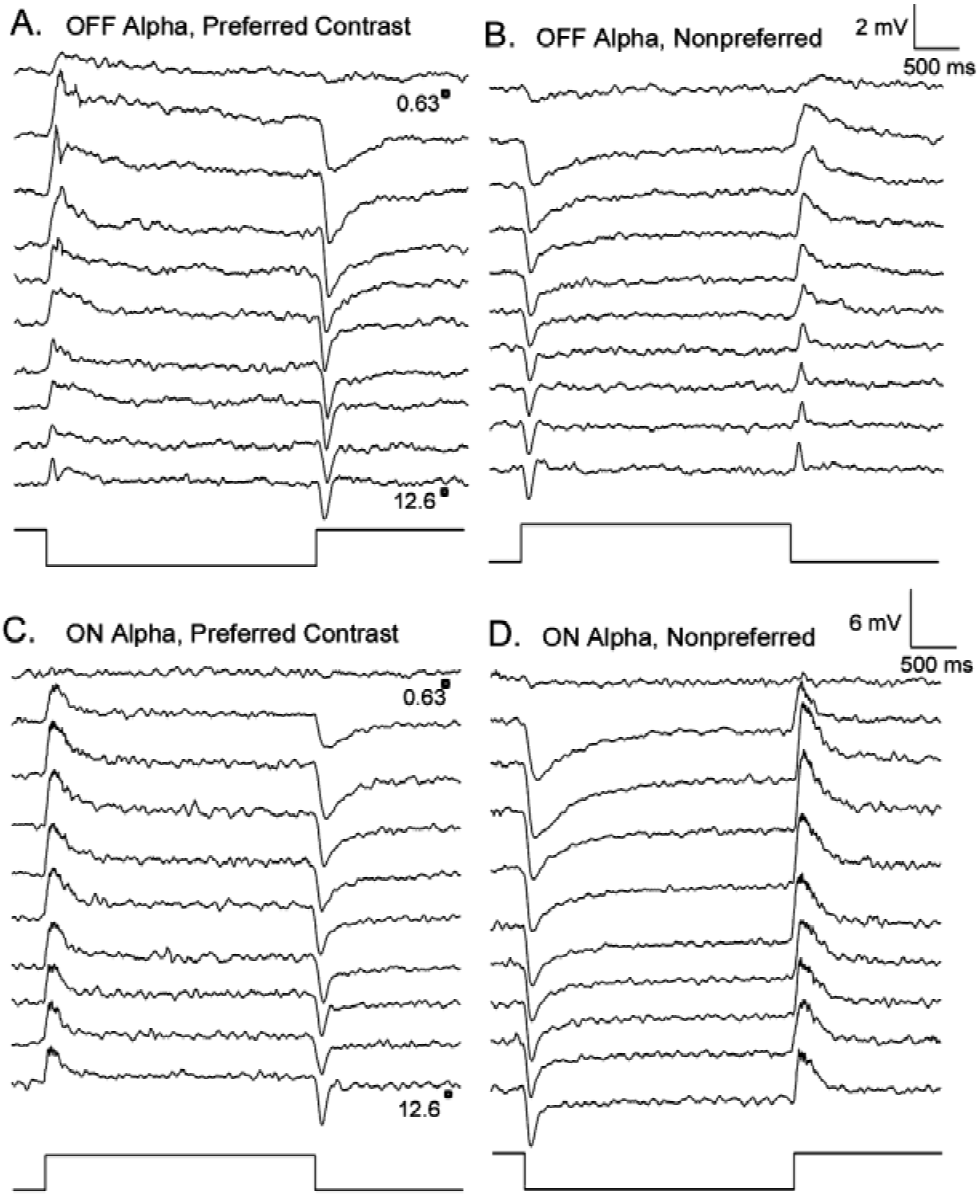

Fig. 2. Averaged and filtered responses of ON and OFF cells to preferred and nonpreferred light stimuli of increasing diameter. Stimuli were centered on the cell and ranged from 0.6 deg to 12.6 deg, increasing in increments of 1.3 deg. Stimulus duration and period were 3 and 6 s, respectively. (A) OFF cell presented with dark spots (preferred contrast) to produce an excitatory response at stimulus onset and an inhibitory response at stimulus offset. Maximal area of depolarization and hyperpolarization noted at 1.96 deg and 3.29 deg, respectively. $V_r = -67$ mV. (B) Same cell in A presented with light spots (nonpreferred contrast) to produce inhibition at stimulus onset and an excitatory response with stimulus offset. Maximal depolarization and hyperpolarization noted at 1.96 deg for both. $V_r = -68$ mV. (C) ON cell presented with light spots (preferred contrast). Maximal depolarization and hyperpolarization noted at 3.29 deg for both. $V_r = -70$ mV. (D) Same cell in C presented with dark spots (nonpreferred contrast). Maximal depolarization and hyperpolarization noted at 4.62 deg and 3.29 deg, respectively. $V_r = -69$ mV.

hyperpolarizations evoked by extinguishing stimuli of preferred contrast, but similar data were obtained for hyperpolarizations evoked by the onset of nonpreferred stimuli.

Bath application of picrotoxin (PTX, 50–100 μM in Ames), or SR-95531 (6 μM) blockers of ionotropic $GABA_{A,C}$ and $GABA_A$ receptors (respectively), largely abolished the size selectivity of the hyperpolarizing mechanism [Fig. 3B(ii)] by preferentially enhancing the response to larger spots. No differences were observed in the effects of PTX or SR-95531, so these data have been pooled for population analyses. The population data show that under picrotoxin, the largest spots tested evoked hyperpolarizations fully 75% as large as the maximal response (Fig. 3C, inverted triangles), whereas under control conditions the corresponding value was only 25% of the maximum. The enhanced hyperpolarization recorded under picrotoxin was essentially eliminated by further addition of strychnine [Fig. 3A(ii); dark gray, Fig. 3C, squares]. Similar data were obtained from analysis of the peak rather than integral hyperpolarization (Fig. 3D). Taken together,

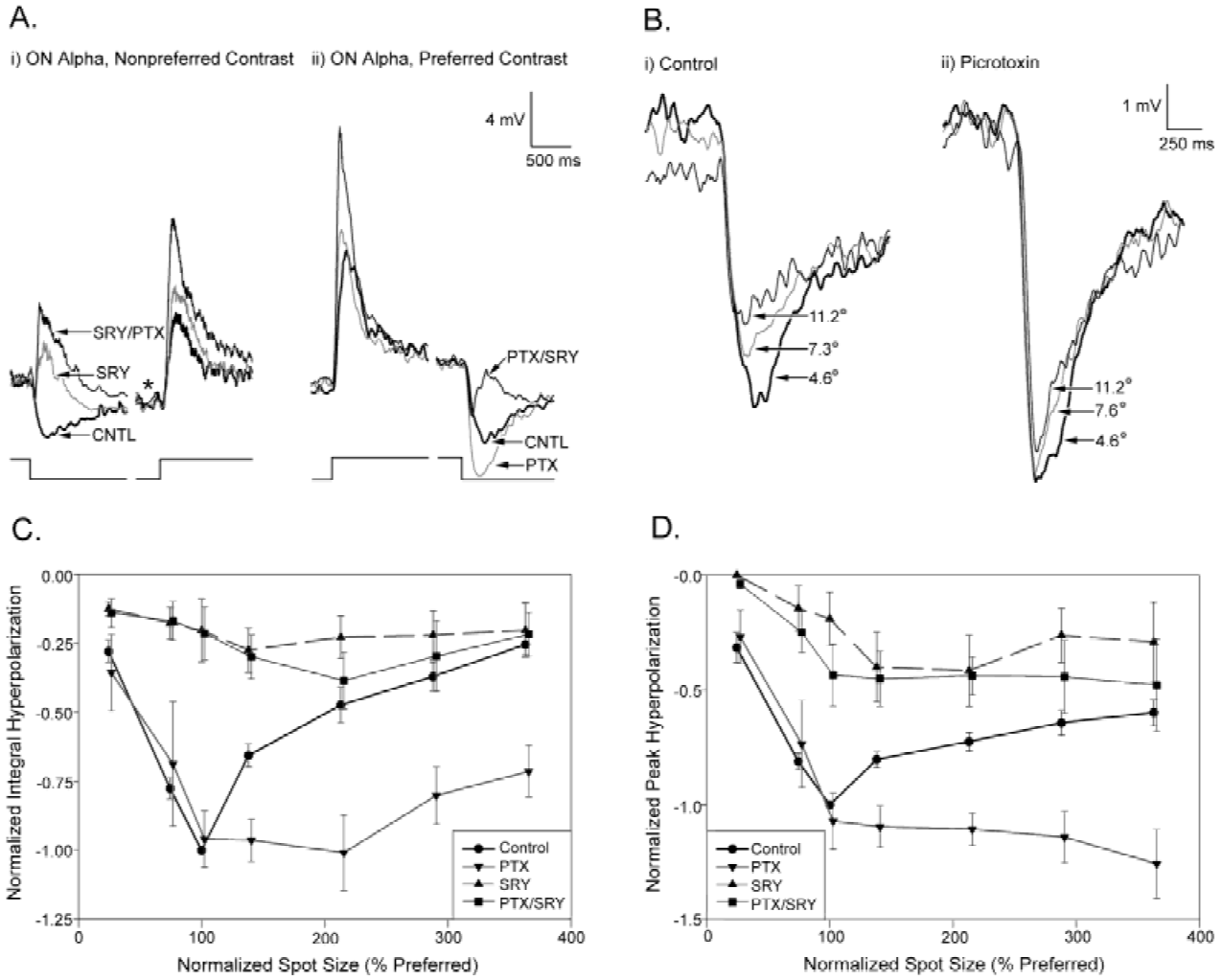

Fig. 3. Pharmacology of the depolarization and hyperpolarization. (A) Light responses of two ON cells at the spot size which produced the maximal area of hyperpolarization in nonpreferred (i; 3.29 deg) and preferred (ii; 4.62 deg) contrast (traces averaged and filtered). Order of application in (i) was control (thick black), SRY (grey) and PTX/SRY (thin black). $V_r = -62$ mV. Order of drug application in (ii) was control (thick black), PTX (grey), and PTX/SRY (thin black). $V_r = -59$ mV. Stimulus duration and period were 3 and 6 s, respectively. Asterisk in (i) indicates sustained, strychnine-insensitive component of the hyperpolarization. (B) PTX eliminates the roll-off of the hyperpolarization. Magnification of the hyperpolarization in Fig. 3A(i) with inclusion of larger spot sizes for control (i) and PTX (ii). (C) Summary of the effects of spot size and of inhibitory antagonists on the hyperpolarization evoked by extinction of a preferred contrast stimulus. The area of the hyperpolarization was obtained by integrating light-evoked membrane voltages more negative than the resting membrane voltage (see Fig. 1 and Methods). This area was normalized by expressing it as a fraction of the maximal hyperpolarization in control recordings. The depolarizing potential sometimes observed during strychnine application made no direct contribution to this measure of hyperpolarization. Spot size is expressed as a percentage of the spot size which produced the maximal area of hyperpolarization in control and was then binned to allow for calculation of standard error. Control (circles; $n = 14$), GABAergic blockade (inverted triangles; $n = 6$), SRY (triangles; $n = 4$), and PTX/SRY (squares, $n = 8$) are included. PTX and PTX/SRY traces are slightly offset to facilitate interpretation. Maximal (100%) hyperpolarization observed at an average spot size of 4.17 deg ± 1.46 deg. (D) Summary graph of the peak hyperpolarization normalized to control and plotted as a function of spot size. Spot size was expressed as a percentage of the spot size which produced the maximal amplitude of hyperpolarization in control. The remainder of the graph was constructed as for Fig. 3C. Note that the optimal spot size for peak hyperpolarization is slightly larger than that of integral/area hyperpolarization so comparability between C and D is only approximate. Maximal (100%) peak hyperpolarization observed at an average spot size of 4.77 deg ± 2.27 deg.

these data suggest that glycinergic inhibition is a necessary component of the circuitry underlying the transient hyperpolarizing light response, while ionotropic GABAergic inhibition helps to shape its size selectivity. The sustained component of hyperpolarization observed during nonpreferred stimulus presentation was not affected by application of PTX or SRY and thus likely represents a sustained reduction in excitatory input.

A secondary depolarization evoked by nonpreferred contrast steps

When the transient hyperpolarization evoked by nonpreferred contrast steps was largely blocked with strychnine, we frequently observed a secondary transient depolarization in its place (e.g. Figs. 3A(i) & 3A(ii)). Under these conditions, the cell had ac-

quired, in essence, an ON–OFF receptive-field center, though the ON-center response remained dominant. In some cells, the same phenomenon could be observed in control medium when using large test spots (Figs. 4A & 4B), presumably because these extended stimuli act much like strychnine to attenuate the hyperpolarization, which otherwise masks this depolarization (see also Fig. 5). The secondary depolarization persisted, and could even be enhanced, by simultaneous bath application of strychnine, picrotoxin (Fig. 3A), and additional 100 μM hexamethonium bromide, a potent antagonist of nicotinic acetylcholine receptors ($n = 2$, data not shown).

Discussion

These data characterize the behavior of a transient hyperpolarization that can be evoked in cat alpha cells by luminance steps in their receptive fields opposite those preferred by the center mechanism. On the basis of the present evidence, we propose that the transient hyperpolarization reflects inhibitory input from glycinergic amacrine cells to bipolar cell terminals presynaptic to alpha cells, to the alpha cell itself, or both. Our data also demonstrate that the glycinergic amacrine cells involved are spatially selective, being subject to surround inhibition from wide-field GABAergic amacrine cells.

The role of glycinergic amacrine cells

The transient hyperpolarization exhibited by alpha cells in response to nonpreferred luminance steps was largely abolished by the selective glycine antagonist strychnine (Fig. 3; see also Fig. 9B of Freed, 2000). This indicates that the transient hyperpolarization results largely from an active inhibitory process. It cannot be

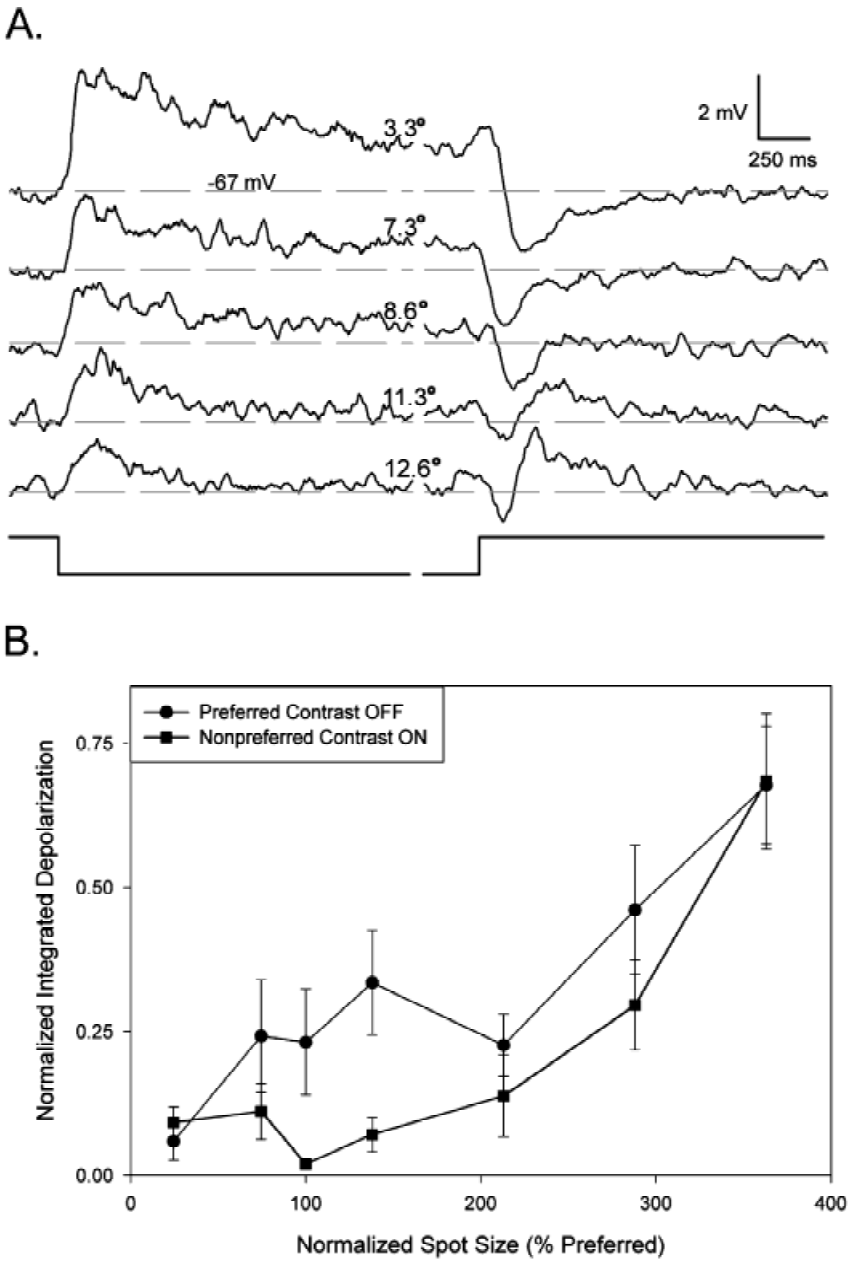

Fig. 4. Analysis of the secondary depolarization. (A) Averaged and filtered responses of an OFF cell presented with different size spots of preferred contrast (dark spot). Note the presence of a secondary depolarization after stimulus offset for the largest two stimuli presented. Stimulus duration and period were 3 and 6 s, respectively. $V_r = -67$ mV. (B) Summary graph of the area of secondary depolarization normalized to maximal during nonpreferred luminance changes under control situations. This was performed for spots of both preferred (circles; $n = 7$) and non-preferred (squares; $n = 4$) contrast. Note that a 100% maximal depolarization is not observed in this figure as cells with smaller receptive fields have multiple values included in our largest bin.

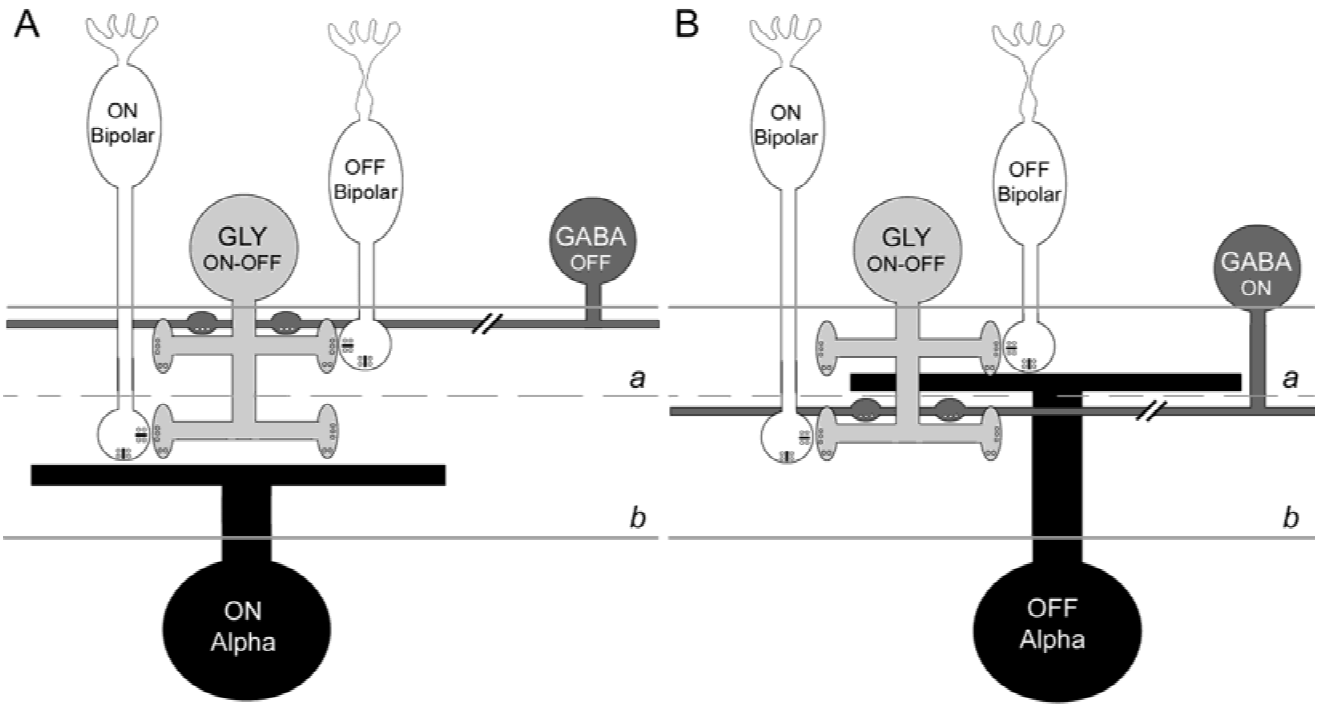

Fig. 5. Diagram of retinal circuit. (A) Circuitry for the ON pathway. Bipolar cells (ON & OFF) receive input from photoreceptors and horizontal cells (not shown) and feedforward onto the dendrites of amacrine and ganglion cells in the inner plexiform layer. A small-field bistratified glycinergic cell (GLY) receives input from both ON and OFF varieties of bipolar cell and provides feedback inhibition to bipolar cell terminals and feedforward alpha cell inhibition. Wide-field GABAergic amacrine cells stratifying in either ON or OFF sublaminae receive input from the corresponding bipolar cells and feedforward to the glycinergic amacrine cells providing them with an antagonistic surround in both IPL strata (for clarity, only one GABAergic cell is presented in each panel). See text for further description of how this circuit might function. (B) Circuitry of the OFF pathway.

explained simply on the basis of withdrawal of excitation from the presynaptic bipolar cells, although this is the likely explanation for the earliest phase of the transient hyperpolarization (seen in Fig. 3A(ii), PTX/SRY) and for the very sustained hyperpolarization (Fig. 3A(i), *), both of which were insensitive to strychnine. The most likely site of action of the glycinergic process is the IPL, since the vast majority of glycinergic interneurons of cat retina are amacrine cells with processes confined to the IPL. However, there are a small number of glycinergic interplexiform cells in the cat retina (Pow & Hendrickson, 1999), and a contribution from these cannot be excluded.

Two lines of evidence suggest that this glycinergic mechanism acts at least partly at a site presynaptic to the recorded alpha cell, presumably at the level of bipolar terminals. First, ionic considerations make it unlikely that direct glycinergic inhibition of the alpha cell alone could produce the observed hyperpolarization. Activation of glycine receptors on the alpha cell membrane should selectively increase its chloride permeability and drive its membrane potential toward the chloride equilibrium potential, which was −57 mV under our recording conditions. Because this is near the resting potential of the recorded alpha cells, glycinergic inhibition of these cells should have produced little change in membrane potential (shunting inhibition) rather than the frank hyperpolarization observed. Second, the transient hyperpolarization evoked by nonpreferred contrast steps was not associated with a measurable decrease in alpha-cell input resistance, as probed with a train of brief current pulses applied during and after the light response ($n = 3$, data not shown). A reduction in input resistance would be expected were the hyperpolarization mediated entirely by direct postsynaptic inhibition.

The foregoing interpretation is partly consistent with observations of Demb et al. (2001*b*; their Fig. 3B). They found that a dimming-evoked hyperpolarization in a guinea pig ON alpha cell had a reversal potential near 0 mV, suggestive of a disfacilitatory (presynaptic inhibitory) mechanism. A substrate for such presynaptic glycinergic inhibition is to be found in the presence of glycine receptors on bipolar axon terminals (Wässle et al., 1998).

While these data strongly implicate presynaptic, feedback inhibition of bipolar input to the alpha cell's response to nonpreferred contrast steps, they do not exclude some contribution from a feedforward glycinergic input to the ganglion cell itself. For example, alpha ganglion cells receive synaptic contacts from glycinergic amacrine cells (Freed & Sterling, 1988) and possess functional glycine receptors (Cohen et al., 1994; Koulen et al., 1996). Further, Demb et al. (2001*b*) reported, in contrast to their results for the ON alpha cell, that the light evoked hyperpolarization in an OFF alpha cell reversed near −100 mV, suggesting a postsynaptic inhibitory mechanism. Further experimentation will be required to determine the balance of presynaptic and postsynaptic mechanisms contributing to the responses of alpha cells to nonpreferred contrast steps.

Properties of the glycinergic amacrine cells

In mammalian retina, glycinergic amacrine cells have narrow dendritic fields (e.g. Vaney, 1990; Menger et al., 1998) and thus,

presumably, small receptive fields. This is broadly consistent with the present evidence that in alpha cells the maximum hyperpolarization for nonpreferred contrast steps is evoked by relatively small stimuli. However, closer scrutiny reveals what may seem a discrepancy in spatial scale. Whereas the stimulus evoking the largest hyperpolarization is roughly comparable in size to the alpha cell's receptive-field center (~4 deg for our cells), the receptive-field dimensions of glycinergic amacrine cells are presumably substantially smaller (<0.5 deg, assuming a spatial correspondence with dendritic-field dimensions of <100 μm in diameter; Menger et al., 1998). In fact, however, this discrepancy is to be expected. The alpha-cell hyperpolarization reflects the spatially integrated influences of all the glycinergic amacrine cells distributed throughout the alpha-cell's dendritic arbor. One way to probe the dimensions of the glycinergic neurons' receptive fields is to ask how far outside the alpha-cell's dendritic field a stimulus can be and still evoke the hyperpolarization. Though we have not addressed this question directly, we did find that spots evoking maximal hyperpolarization are on average only slightly larger than the alpha-cell dendritic field, suggesting that the inhibitory neurons involved have relatively narrow fields.

The data also have implications for the dendritic stratification of these glycinergic amacrine cells and implies that they deploy presynaptic dendrites in the same sublayer as the alpha cell and its presynaptic bipolar cells (i.e. in the ON sublayer for ON alphas, and in the OFF sublayer for OFF alphas). Note, however, that the hyperpolarization is triggered by luminance changes opposite those exciting bipolar cells in this sublayer. This implies that the glycinergic amacrines receive excitatory bipolar input in the IPL sublayer opposite that occupied by the alpha-cell dendrites (i.e. in the OFF sublayer for ON alphas, and in the ON sublayer for OFF alphas). In other words, these glycinergic amacrines seem very likely to be either bistratified or broadly stratified in both the ON and OFF sublayers. There is ample precedent for amacrine-cell-mediated inhibitory crosstalk between the ON and OFF sublaminae of mammalian retina (e.g. Bloomfield & Miller, 1986; Roska & Werblin, 2001) and in cat retina ON-channel inhibition of OFF ganglion cells has been shown to be glycinergic (Wässle et al., 1986). Many glycinergic amacrine cells do arborize in both ON and OFF sublayers (Wright et al., 1997; Menger et al., 1998).

If the glycinergic amacrine cells responsible for the transient alpha cell hyperpolarization are indeed bistratified, it is possible that they receive excitatory bipolar input in both of these sublayers, that is, that they are ON–OFF amacrine cells. If so, their inhibitory contacts would attenuate alpha-cell depolarization to preferred contrast steps in addition to hyperpolarizing the cell during nonpreferred steps. Consistent with this inference, the excitatory center response is augmented by strychnine in some alpha cells [Figs. 3A(i) & 3A(ii)]. However, this effect is not evident in all cells (e.g. see Fig. 9B of Freed, 2000) and in any case could reflect contributions from glycinergic amacrines distinct from those mediating the hyperpolarization.

GABAergic modulation of the glycinergic mechanism

The hyperpolarization of alpha cells by nonpreferred luminance steps is evoked much more effectively by spots than by wide-field stimuli. This implies that the glycinergic neurons mediating the hyperpolarization are subject to surround antagonism. This spatial antagonism seems to be established largely by a GABAergic inhibitory circuit in the IPL, since it is largely abolished by picrotoxin. The small residual size dependence that persists under picrotoxin (Fig. 3C) may be attributable to non-GABAergic horizontal cell circuits mediating surround antagonism in the bipolar cells driving the glycinergic cell. At least in goldfish retina, feedback from horizontal cells to photoreceptors may involve an ephaptic mechanism which shifts the activation curve of photoreceptor voltage-gated Ca^{2+} channels (Kamermans et al., 2001).

A clear precedent exists for GABAergic input to, and surround antagonism in, a narrow-field bistratified glycinergic amacrine cell, namely the DAPI-3 cell of rabbit retina (Bloomfield, 1992; Wright et al., 1997; Zucker & Ehinger, 1998; Kim et al., 2002). The spatial antagonism of glycinergic cells by GABAergic cells is also consistent with previous reports of serial inhibitory influences on ganglion-cell light responses in amphibian retina (Zhang et al., 1997; Cook et al., 2000). Of course, the interpretation of neurotransmitter antagonist effects in serial inhibition is very complex. Removal of glycinergic inhibition with SRY not only affects the alpha cell recorded, but also likely affects bipolar cell output to other amacrine cells (e.g. GABAergic cells) which may in turn affect the responsiveness of the alpha cell. Thus, the effects of any individual antagonist on ganglion-cell light responses may not be limited to the targeted neurotransmitter.

The magnitude of the GABAergic attenuation of the glycinergic hyperpolarization increases with stimulus size up to the largest we could generate (~12-deg diameter). This implies that the GABAergic amacrine cells responsible for this lateral inhibitory influence have large receptive fields and can transmit their influence a considerable distance across the retina. This is in keeping with the wide-field dendritic arbors of mammalian GABAergic amacrine cells and evidence that many such cells have extensive intraretinal axonal projections (Vaney, 1990; MacNeil et al., 1999). In amphibian retina, however, the opposite organization has been described (Yang et al., 1991, Cook et al., 1998, Roska et al., 1998, but see also Deng et al., 2001 for an alternate view). The GABAergic suppressive mechanism we have observed is seemingly triggered by the same sign of luminance change as evokes the glycinergic mechanism, namely a nonpreferred luminance step from the perspective of the alpha cell. This implies that the wide-field GABAergic amacrines involved stratify at least partly in the IPL sublayer opposite that in which the alpha cell stratifies.

Fig. 5 summarizes the main elements of the foregoing analysis in a schematic model of the circuitry as applied to ON (Fig. 5A) and OFF (Fig. 5B) alpha cells. The ON alpha cell receives excitatory input from ON bipolars in the ON sublayer of the IPL and inhibitory input from the processes of an ON–OFF glycinergic amacrine cell which also stratify in the same sublamina. The bipolar terminals also receive glycinergic inhibitory contacts from bistratified ON–OFF amacrine cells. The glycinergic cells, in turn, receive ionotropic GABAergic inhibition from wide-field OFF amacrine cells (or possibly ON–OFF amacrines, not illustrated). Though alpha cells also receive direct GABAergic inhibitory inputs (Cohen et al., 1994; Koulen et al., 1996; Owczarzak & Pourcho, 1999), these synapses have been omitted from the model circuit as our data do not directly address their roles.

Introduction of a dark stimulus into the receptive field of the ON alpha (a nonpreferred contrast step) hyperpolarizes the alpha cell by decreasing glutamate release from the bipolar cells that drive it (disfacilitation). This occurs through two distinct mechanisms, one in each of the plexiform layers. In the outer retina, the dimming generates a sustained hyperpolarization of the ON bipolars by increasing glutamate release from the photoreceptors and activating metabotropic glutamate receptors on the ON bipolar dendrites. In the inner retina, the dimming triggers a transient

inhibition of the axon terminals of the same bipolar cells through OFF-channel excitation of glycinergic amacrine cells. These glycinergic cells, which may also synapse directly onto the ON alpha, are most strongly recruited when the dimming is fairly localized, and therefore ineffective in activating the wide-field GABAergic amacrines. When dark stimuli are large, by contrast, the GABAergic neurons are recruited, suppressing the response of the glycinergic amacrines and reducing the transient hyperpolarizing mechanism. The same model can be adapted for OFF alpha cells by simply inverting the position of each of the circuit elements in the ON or OFF sublayer of the IPL (Fig. 5B). A similar pattern of circuitry was proposed by Müller et al. (1992) in their study of GABAergic inhibition of cat brisk-transient (Y type) and brisk-sustained (X type) ganglion cells. Our data confirm their model for inhibition of OFF alpha cells, extend it to ON alpha cells, and provide data regarding the relative sizes of the GABAergic and glycinergic cells involved. Finally, Roska et al. (1998) proposed a similar sort of circuitry in the amphibian retina except that the neurochemical identities of the wide-field and narrow-field amacrine cells were reversed.

Relevance to models of spatial nonlinearity of Y-cell receptive fields

Alpha cells (i.e. Y-cells) exhibit prominent nonlinearities of spatial summation, attributable to the influence of "rectifying subunits" with receptive fields much smaller than the Y-cell itself (Hochstein & Shapley, 1976*b*). For example, high spatial-frequency drifting sinusoidal contrast gratings can elevate mean discharge rate in Y-cells without modulating the firing frequency at the temporal frequency of the stimulus (Enroth-Cugell & Robson, 1966; Hochstein & Shapley, 1976*a*). Similarly, stationary counterphasing gratings can evoke response modulation at twice the frequency of the stimulus (frequency doubling). The rectifying subunits are thought to correspond to the receptive fields of bipolar cells presynaptic to the Y-cell. Subunit nonlinearity is thought to reflect a nonlinearity in the relationship between luminance and glutamate release in the bipolar cells' response to contrast steps. This might occur, for example, if the bipolar cell light response is relatively transient (DeVries, 2000; Awatramani & Slaughter, 2000) and its resting rate of glutamate release is low (Freed, 2000). Nonlinearities within the Y-cell receptive-field center presumably reflect mainly direct excitatory input from such rectifying bipolar cells onto the Y-cell. However, spatially nonlinear influences on the Y-cell can also be evoked from far outside the classical receptive field (McIlwain, 1964; Thibos & Werblin, 1978; Enroth-Cugell & Jakiela, 1980; Passaglia et al., 2001) and these appear to involve wide-field spiking amacrine cells as critical circuit elements (Demb et al., 1999, 2001*b*).

Within the receptive-field center, the glycinergic mechanism identified here appears to partly counteract this rectification in bipolar output and thus to limit the extent of alpha-cell nonlinearity. Under normal circumstances, the depolarization caused by high-contrast spots in the alpha-cell receptive field is two-fold to five-fold larger for preferred-contrast steps than the hyperpolarization caused by nonpreferred steps (Demb et al., 2001; see their Fig. 5). Because the hyperpolarization is largely supported by the glycinergic circuit identified here, the imbalance would be much more pronounced in the absence of this inhibitory network. Note that if the relevant glycinergic amacrine cells are ON–OFF center, their "linearizing" effect on bipolar output would include a second component, namely, limiting the bipolar glutamate release evoked by preferred luminance steps.

The present data reveal a further nonlinearity in the excitatory input to the alpha cell that has received little previous attention. This is the secondary depolarization of the alpha cell by nonpreferred luminance steps when the glycinergic mechanism is suppressed either pharmacologically or by the use of large stimuli (acting *via* the GABAergic circuit discussed here). Though we have not analyzed this response in detail, we note that it survives blockade of ionotropic inhibition as well as nicotinic excitation in the IPL. A similar effect has been noted in salamander ganglion cells for annular stimuli in the presence of tetrodotoxin or combined application of strychnine and PTX (Cook & McReynolds, 1998). The origins of this response are presently unclear. It might reflect a property of the bipolar input, because bipolar cells can express weakly biphasic (ON–OFF) responses under some circumstances (Nelson & Kolb, 1983; Wu et al., 2000; Dacey et al., 2000). Another potential mechanism is electrical coupling between alpha cells and amacrine cells (Brivanlou et al., 1998). Alpha cells are well known to be dye-coupled to wide-field amacrine cells in several mammalian species including the cat, and some of these are thought to have transient ON–OFF light responses (Vaney, 1991; Dacey & Brace, 1992; Penn et al., 1994, Jacoby et al., 1996; Xin & Bloomfield; 1997; Schubert & Weiler, 2002). Whatever its origin, the glycinergic circuitry outlined here appears to override this secondary excitatory response under most stimulus conditions, in effect, further linearizing the alpha-cell light response.

As noted above, luminance modulation well outside the classical receptive field can modulate alpha-cell discharge rate by a mechanism that is spatially nonlinear. The modulation is excitatory when the remote stimulus contains low spatial frequencies and inhibitory when it contains high spatial frequencies (Passaglia et al., 2001). These long-range modulatory effects appear to be dependent on wide-field spiking amacrine cells, because they are abolished by tetrodotoxin (Cook et al., 1998; Cook & McReynolds, 1998; Demb et al., 1999). The amacrine cells responsible for these effects could be the same as the wide-field GABAergic amacrines in our model (Fig. 5) mediating the surround antagonism of the glycinergic amacrine cells. Stimuli of low spatial frequency should effectively excite these GABAergic amacrines, which through their broad axonal arbors would evoke widespread inhibition of the glycinergic amacrines and, thus, far-reaching disinhibition of bipolar axon terminals and/or alpha cells. This general reduction in glycinergic inhibition will increase the input resistances of one or both postsynaptic cell types and therefore increase the gain for signals entering this pathway (Fig. 5). The inhibitory effect on alpha cells induced by remote stimuli of high spatial frequency (Passaglia et al., 2001) could indicate that the GABAergic amacrine cells proposed in the model circuit (Fig. 5) receive reciprocal inhibitory input from narrow-field glycinergic amacrine cells (not shown). High-frequency stimuli presented in the periphery would lead to an increase in glycinergic release local to the recorded alpha cell (*via* a reduction in GABA release from wide-field cells), and a net decrease in input resistance, leading to a reduction in the gain of this pathway. This proposed scheme of interacting inhibitory networks of differing spatial scales may underlie aspects of spatial-frequency tuning and adaptation among retinal ganglion cells.

Acknowledgments

This research was supported by NIH grants R01 EY06108 and R01 EY12793 and training grant T32 MH19118.

References

Awatramani, G.B. & Slaughter, M.M. (2000). Origin of transient and sustained responses in ganglion cells of the retina. *Journal of Neuroscience* **20**, 7087–7095.

Bishop, P.O., Kozak, W. & Vakkur, J. (1962). Some quantitative aspects of the cat's eye: Axis and plane of refrence, visual field co-ordinates and optics. *Journal of Physiology* (London) **163**, 466–502.

Bloomfield, S.A. (1992). Relationship between receptive and dendritic field size of amacrine cells in the rabbit retina. *Journal of Neurophysiology* **68**, 711–725.

Bloomfield, S.A. & Miller, R.F. (1986). A functional organization of ON and OFF pathways in the rabbit retina. *Journal of Neuroscience* **6**, 1–13.

Boycott, B.B. & Wässle, H. (1974). The morphological types of ganglion cells of the domestic cat's retina. *Journal of Physiology* (London) **240**, 397–419.

Brivanlou, I.H., Warland, D.K. & Meister, M. (1998). Mechanisms of concerted firing among retinal ganglion cells. *Neuron* **20**(3), 527–539.

Cohen, E.D., Zhou, Z.J. & Fain, G.L. (1994). Ligand-gated currents of alpha and beta ganglion cells in the cat retinal slice. *Journal of Neurophysiology* **72**, 1260–1269.

Cook, J.E. (1997). Getting to grips with neuronal diversity: What is a neuronal type? In *Development and Organization of the Retina: From Molecules to Function*, ed. Chalupa, L.M. & Finlay, B.L., pp. 91–120. New York: Plenum Press.

Cook, P.B. & McReynolds, J.S. (1998). Lateral inhibition in the inner retina is important for spatial tuning of ganglion cells. *Nature Neuroscience* **1**, 714–719.

Cook, P.B., Lukasiewicz, P.D. & McReynolds, J.S. (1998). Action potentials are required for the lateral transmission of glycinergic transient inhibition in the amphibian retina. *Journal of Neuroscience* **18**, 2301–2308.

Cook, P.B., Lukasiewicz, P.D. & McReynolds, J.S. (2000). GABA(C) receptors control adaptive changes in a glycinergic inhibitory pathway in salamander retina. *Journal of Neuroscience* **20**, 806–812.

Dacey, D.M. (1999). Primate retina: Cell types, circuits and color opponency. *Progress in Retinal and Eye Research* **18**, 737–763.

Dacey, D.M. & Brace, S. (1992). A coupled network for parasol but not midget ganglion cells in the primate retina. *Visual Neuroscience* **9** (3–4), 279–290.

Dacey, D., Packer, O.S., Diller, L., Brainard, D., Peterson, B. & Lee, B. (2000). Center surround receptive field structure of cone bipolar cells in primate retina. *Vision Research* **40**, 1801–1811.

Demb, J.B., Haarsma, L., Freed, M.A. & Sterling, P. (1999). Functional circuitry of the retinal ganglion cell's nonlinear receptive field. *Journal of Neuroscience* **19**, 9756–9767.

Demb, J.B., Zaghloul, K. & Sterling, P. (2001*a*). Cellular basis for the response to second-order motion cues in Y retinal ganglion cells. *Neuron* **32**, 711–721.

Demb J.B., Zaghloul, K., Haarsma, L. & Sterling, P. (2001*b*). Bipolar cells contribute to nonlinear spatial summation in the brisk-transient (Y) ganglion cell in mammalian retina. *Journal of Neuroscience* **21**, 7447–7454.

Deng, P., Cuenca, N., Doerr, T., Pow, D.V., Miller, R. & Kolb, H. (2001). Localization of neurotransmitters and calcium binding proteins to neurons of salamander and mudpuppy retinas. *Vision Research* **41**, 1771–1783.

DeVries, S.H. (2000). Bipolar cells use kainate and AMPA receptors to filter visual information into separate channels. *Neuron* **28**, 847–856.

Enroth-Cugell, C. & Jakiela, H.G. (1980). Suppression of cat retinal ganglion cell responses by moving patterns. *Journal of Physiology* (London) **302**, 49–72.

Enroth-Cugell, C. & Robson, J.G. (1966). The contrast sensitivity of retinal ganglion cells of the cat. *Journal of Physiology* (London) **187**, 517–552.

Enroth-Cugell, C., Hertz, B.G. & Lennie, P. (1977). Convergence of rod and cone signals in the cat's retina. *Journal of Physiology* (London) **269**, 297–318.

Freed, M.A. (2000). Rate of quantal excitation to a retinal ganglion cell evoked by sensory input. *Journal of Neurophysiology* **83**, 2956–2966.

Freed, M.A. & Sterling, P. (1988). The ON-alpha ganglion cell of the cat retina and its presynaptic cell types. *Journal of Neuroscience* **8**, 2303–2320.

Hamill, O.P., Marty, A., Neher, E., Sakmann, B. & Sigworth, F.J. (1981). Improved patch-clamp techniques for high-resolution current recording from cells and cell-free membrane patches. *Pflügers Archive* **391**, 85–100.

Hochstein, S. & Shapley, R.M. (1976*a*). Quantitative analysis of retinal ganglion cell classifications. *Journal of Physiology* (London) **262**, 237–264.

Hochstein, S. & Shapley, R.M. (1976*b*). Linear and nonlinear spatial subunits in Y cat retinal ganglion cells. *Journal of Physiology* (London) **262**, 265–284.

Jacoby, R., Stafford, D., Kouyama, N. & Marshak, D. (1996) Synaptic inputs to ON parasol ganglion cells in the primate retina. *Journal of Neuroscience* **16** (24), 8041–8056.

Kamermans, M., Fahrenfort, I., Schultz, K., Janssen-Bienhold, U., Sjoerdsma, T. & Weiler, R. (2001). Hemichannel-mediated inhibition in the outer retina. *Science* **292**, 1178–1180.

Kim, I.-B., Lee, E.-J., Oh, S.-J., Park, C.-B., Pow, D.V. & Chun, M.-H. (2002). Light- and electron-microscopic analysis of aquaporin 1-like immunoreactive amacrine cells in the rat retina. *Journal of Comparative Neurology* **452**, 178–191.

Koulen, P., Sassoe-Pognetto, M., Grünert, U. & Wässle, H. (1996). Selective clustering of GABA(A) and glycine receptors in the mammalian retina. *Journal of Neuroscience* **16**, 2127–2140.

MacNeil, M.A., Heussy, J.K.,, Dacheux, R.F., Raviola, E. & Masland, R.H. (1999) The shapes and numbers of amacrine cells: Matching of photofilled with Golgi-stained cells in the rabbit retina and comparison with other mammalian species. *Journal of Comparative Neurology* **413**, 305–326.

McIlwain, J.T. (1964). Receptive fields of optic tract axons and lateral geniculate cells: Peripheral extent and barbiturate sensitivity. *Journal of Neurophysiology* **27**, 1154–1173.

Menger, N., Pow, D.V. & Wässle, H. (1998). Glycinergic amacrine cells of the rat retina. *Journal of Comparative Neurology* **401**, 34–46.

Müller, F., Boos, R. & Wässle, H. (1992). Actions of GABAergic ligands on brisk ganglion cells in the cat retina. *Visual Neuroscience* **9**, 415–425.

Neher, E. (1992). Correction for liquid junction potentials in patch-clamp experiments. *Methods in Enzymology* **207**, 123–131.

Nelson, R. & Kolb, H. (1983). Synaptic patterns and response properties of bipolar and ganglion cells in the cat retina. *Vision Research* **23**, 1183–1195.

O'Brien, B.J., Isayama, T., Richardson, R. & Berson, D.M. (2002). Intrinsic physiological properties of cat retinal ganglion cells. *Journal of Physiology* (London) **538**, 787–802.

Owczarzak, M.T. & Pourcho, R.G. (1999). Transmitter-specific input to OFF-alpha ganglion cells in the cat retina. *Anatomical Record* **255**, 363–373.

Passaglia, C.L., Enroth-Cugell, C. & Troy, J.B. (2001). Effects of remote stimulation on the mean firing rate of cat retinal ganglion cells. *Journal of Neuroscience* **21**, 5794–5803.

Peichl, L. (1991). Alpha ganglion cells in mammalian retinae: Common properties, species differences, and some comments on other ganglion cells. *Visual Neuroscience* **7**, 155–169.

Penn, A.A., Wong, R.O. & Shatz, C.J. (1994). Neuronal coupling in the developing mammalian retina. *Journal of Neuroscience* **14** (6), 3805–3815.

Pow, D.V. & Hendrickson, A.E. (1999). Distribution of the glycine transporter glyt-1 in mammalian and nonmammalian retinae. *Visual Neuroscience* **16**, 231–239.

Pu, M. & Berson, D.M. (1992). A method for reliable and permanent intracellular staining of retinal ganglion cells. *Journal of Neuroscience Methods* **41**, 45–51.

Robinson, D.W. & Chalupa, L.M. (1997). The intrinsic temporal properties of alpha and beta retinal ganglion cells are equivalent. *Current Biology* **7**, 366–374.

Rodieck, R.W. (1998). *The First Steps in Seeing*. Sunderland, Massachusetts: Sinauer Associates.

Rodieck, R.W. & Brening, R.K. (1983). Retinal ganglion cells: Properties, types, genera, pathways and trans-species comparisons. *Brain, Behavior, and Evolution* **23**, 121–164.

Roska, B. & Werblin, F. (2001). Vertical interactions across ten parallel, stacked representations in the mammalian retina. *Nature* **410**, 583–587.

Roska, B., Nemeth, E. & Werblin, F.S. (1998). Response to change is facilitated by a three-neuron disinhibitory pathway in the tiger salamander retina. *Journal of Neuroscience* **18**, 3451–3459.

ROWE, M.H. & STONE, J. (1977). Naming of neurones. Classification and naming of cat retinal ganglion cells. *Brain, Behavior, and Evolution* **14**, 185–216.

SCHUBERT, T. & WEILER, R. (2002). Connexin36 is involved in the coupling pattern of alpha ganglion cells in the mouse retina. *FENS Forum Abstracts* **3**, 60.

STONE, J. (1983) *Parallel Processing in the Visual System*. New York: Plenum Press.

TAYLOR, W.R. & WÄSSLE, H. (1995). Receptive field properties of starburst cholinergic amacrine cells in the rabbit retina. *European Journal of Neuroscience* **7**, 2308–2321.

THIBOS, L.N. & WERBLIN, F.S. (1978). The properties of surround antagonism elicited by spinning windmill patterns in the mudpuppy retina. *Journal of Physiology* (London) **278**, 101–116.

TROY, J.B. & SHOU, T. (2002). The receptive fields of cat retinal ganglion cells in physiological and pathological states: Where we are after half a century of research? *Progress in Retinal and Eye Research* **21**, 263–302.

VANEY, D.I. (1990). The mosaic of amacrine cells in the mammalian retina. In *Progress in Retinal Research*, ed. OSBORNE, J.J. & CHADER, G., pp. 49–100. Oxford, UK: Pergamon.

VANEY, D.I. (1991). Many diverse types of retinal neurons show tracer coupling when injected with biocytin or Neurobiotin. *Neuroscience Letters* **125** (2), 187–190.

WÄSSLE, H. & BOYCOTT, B.B. (1991). Functional architecture of the mammalian retina. *Physiological Reviews* **71**, 447–480.

WÄSSLE, H., SCHAFER-TRENKLER, I. & VOIGT, T. (1986). Analysis of a glycinergic inhibitory pathway in the cat retina. *Journal of Neuroscience* **6**, 594–604.

WÄSSLE, H., KOULEN, P., BRANDSTÄTTER, J.H., FLETCHER, E.L. & BECKER, C.M. (1998). Glycine and GABA receptors in the mammalian retina. *Vision Research* **38**, 1411–1430.

WRIGHT, L.L., MACQUEEN, C.L., ELSTON, G.N., YOUNG, H.M., POW, D.V. & VANEY, D.I. (1997). The DAPI-3 amacrine cells of the rabbit retina. *Visual Neuroscience* **14**, 473–492.

WU, S.M., GAO, F. & MAPLE, B.R. (2000). Functional architecture of synapses in the inner retina: Segregation of visual signals by stratification of bipolar cell axon terminals. *Journal of Neuroscience* **20**, 4462–4470.

XIN, D. & BLOOMFIELD, S.A. (1997). Tracer coupling pattern of amacrine and ganglion cells in the rabbit retina. *Journal of Comparative Neurology* **383** (4), 512–528.

YANG, C-Y., LUKASIEWICZ, P., MAGUIRE, G., WERBLIN, F.S. & YAZULLA, S. (1991). Amacrine cells in the tiger salamander retina: Morphology, physiology, and neurotransmitter identification. *Journal of Comparative Neurology* **312**, 19–32.

ZHANG, J., JUNG, C-S. & SLAUGHTER, M.M. (1997). Serial inhibitory synapses in retina. *Visual Neuroscience* **14**, 553–563.

ZUCKER, C.L. & EHINGER, B. (1998). Gamma-aminobutyric acid A receptors on a bistratified amacrine cell type in the rabbit retina. *Journal of Comparative Neurology* **393**, 309–319.